PHYSICAL REVIEW B **86**, 060406(R) (2012)

Magnetic ordering in bulk MnSi crystals with chemically induced negative pressure

Nadya Potapova,[1] Vadim Dyadkin,[1] Evgeniy Moskvin,[1] Helmut Eckerlebe,[2] Dirk Menzel,[3] and Sergey Grigoriev[1]
[1]*Petersburg Nuclear Physics Institute, Gatchina, 188300 St-Petersburg, Russia*
[2]*Helmholz-Zentrum Geesthacht, 21502 Geesthacht, Germany*
[3]*Technische Universität Braunschweig, D-38106 Braunschweig, Germany*
(Received 8 July 2012; published 13 August 2012)

MnSi crystals with chemically induced negative pressure (doped by less than 1% Ge) have been synthesized by the Czochralski method. X-ray powder diffraction has revealed that the samples are crystallized in the B20 structure, inherent to pure MnSi, without any impurity phases. The lattice constant a is slightly larger than that of undoped MnSi. The samples have a spiral spin structure with the wave vector $|\mathbf{k}| = 0.385$ nm^{-1} at low temperatures. The ordering temperature is enhanced up to $T_C = 39$ K. The critical field H_{C2} shows an increase of about 25% for the doped samples. Close to the critical temperature the A phase occurs. The temperature range of the A phase in the (H-T) phase diagram for the doped compound ranges from $T_A = 27.5$ K, characteristic for pure MnSi, to $T_C = 39$ K in the zero-field cooled (ZFC) regime of magnetization. The magnetic features of the (H-T) phase diagram of the compounds MnSi are reminiscent of those observed for the MnSi thin films on the Si substrate.

DOI: 10.1103/PhysRevB.86.060406 PACS number(s): 61.05.fg, 75.50.Cc, 76.60.Lz

The magnetic and transport properties of MnSi and the relative compounds $Fe_{1-x}Co_xSi$, the noncentrosymmetric cubic magnets with the space group $P2_13$, have been a subject of intensive investigations in recent years. Attention has focused mostly on the following four problems: (i) the quantum phase transition (QPT) observed under applied pressure,[1–6] (ii) the complex nature of the thermal phase transition,[7–12] (iii) the appearance of the A phase in the H-T phase diagram (two-dimensional [2D] structure with **k** perpendicular to **H**),[13–15] and (iv) the crystallographic handedness and spin chirality.[16–19] All these problems are certainly interconnected, although they touch very different fundamental issues in modern condensed-matter physics.

A further aspect of the problems related to MnSi is possible applications of those fundamental physical properties in modern spintronic devices.[20,21] An important parameter of the applicability of these compounds is the ordering temperature T_c, the desirable value of which should be comparable or greater than room temperature. The largest ordering temperature of the B20 compounds is observed for pure FeGe and is equal to 278.6 K.[22] The attempts to change the ordering temperature of the pure bulk compound (MnSi) by chemical substitution (with Fe or Co) has resulted in a decrease of the ordering temperature only.[23–25]

A certain success on the way to increase the ordering temperature in these compounds was recently reported in the synthesis of the epitaxial MnSi (111) thin films.[26–28] The authors had reported on the correlation between the magnetic and structural properties of epitaxial MnSi (111) thin films grown by solid-phase epitaxy on Si (111) substrates. The Si (111) substrate, with a surface unit cell of 3.0% larger than that of MnSi, causes an in-plane tensile strain in the film that is partially relaxed due to the presence of misfit dislocations at the interface. However, the out-of-plane strain has a nonmonotonic dependence on thickness that is attributed to changes in the elastic constants of the film. The thickness dependence of the Curie temperature correlates strongly with strain and reaches a maximum of $T_C = 43$ K, a value that is 46% greater than the bulk value of $T_C = 29.5$ K.

As shown in Ref. 29, the decrease of the lattice parameter of 0.3% under applied pressure results in decrease of the ordering temperature for about 20 K. It is natural to suppose that an increase of the lattice parameter will be followed by the increase of the ordering temperature. In this Rapid Communication we demonstrate that MnSi with chemically induced negative pressure shows an increase of the ordering temperature T_C up to values comparable to those of thin films. We have observed the changes in the critical fields and the wave vector **k** with temperature. In general, a qualitative picture of the magnetic behavior and the characteristic parameters of such samples are comparable to and reminiscent of those of MnSi thin films.[26,27]

The samples were unintentionally grown as a side product in the crystal growth of the pseudobinary compound $MnSi_{1-x}Ge_x$. For the tri-arc Czochralski crystal growth, high-purity components of Mn:Si:Ge were mixed with the proportions of 5:4:1, 5:3:2, and 2:1:1. The mixture was molten in a water-cooled copper crucible under an argon atmosphere with a pressure of 2.5 bar. The heating was provided by three electric arcs. The clockwise-revolving seed crystal was submerged into the oppositely rotating melt. Subsequently, the crystal was slowly drawn out of the melt at the speed of 12 mm/h.

To establish the composition and phase identity of these samples, a careful characterization by scanning electron microscopy and fluorescent x-ray analysis has been performed using a JPRS40-51 electron microscope at the Institute of General and Inorganic Chemistry of Russian Academy of Sciences (RAS). The surface of the MnSi sample looks homogeneous and does not contain any other phases. Chemical element analyses were performed on various parts of the sample. The chemical elements (Mn and Si) have been found to be distributed homogeneously throughout the crystal. It is found that the deficit of Si or Mn as elements in the sample does not exceed 10%, so the sample should be considered as nonstoichiometric $MnSi_{1-x}$ with x within ± 0.10. Small traces of Ge in these crystals do not exceed the value of 1%.

X-ray powder diffraction has been performed using a STOE Stadi MP diffractometer. The analysis of the x-ray powder

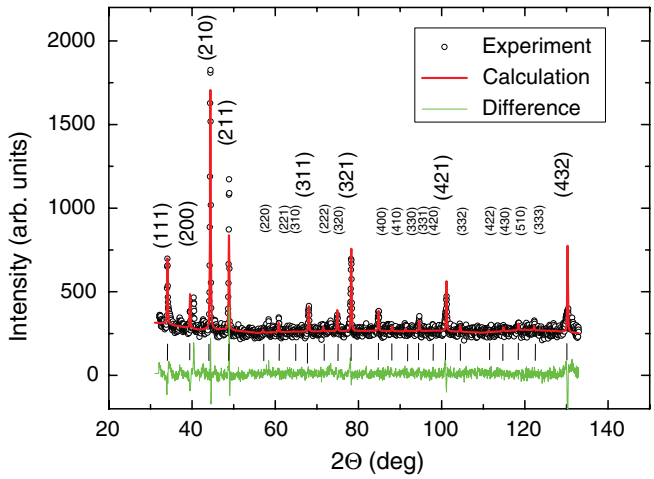

FIG. 1. (Color online) X-ray powder diffraction spectrum of the doped MnSi sample at $T = 293$ K.

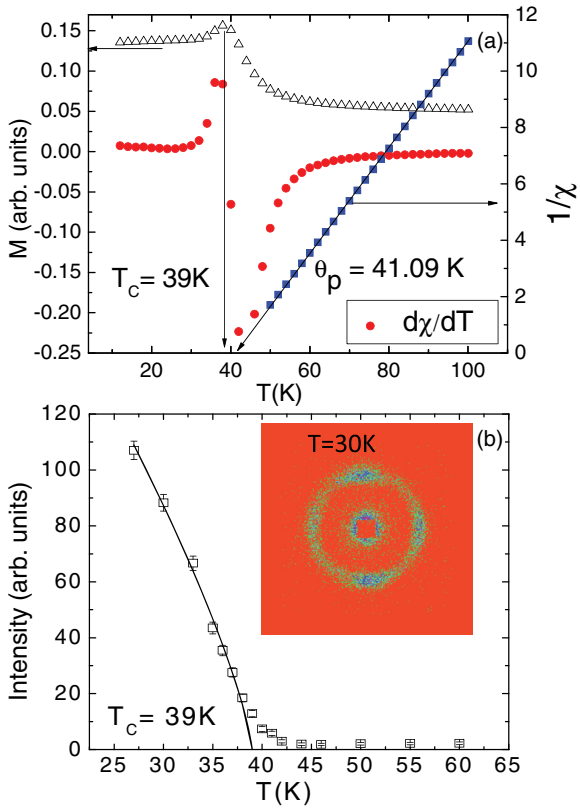

FIG. 2. (Color online) (a) Temperature dependence of the susceptibility χ and its first derivative on temperature $d\chi/dT$ at an applied magnetic field of 5 mT. Additionally the temperature dependence of the reciprocal susceptibility $1/\chi$ is plotted for the paramagnetic range $T > T^*$. (b) Temperature dependence of the integral small-angle neutron scattering (SANS) intensity for the doped MnSi sample at $H = 1$ mT. Inset: Map of the SANS intensity taken at $T = 30$ K.

diffraction spectra has evidenced that all samples show the cubic B20 structure, typical for pure MnSi compound, without any additional phases (See Fig. 1 for example). The lattice constant of these samples at room temperature $a = 4.575(1)$ Å is slightly larger than the lattice parameter $a = 4.558(1)$ Å of an ideal MnSi crystal. It can be concluded that the obtained crystals are polycrystalline MnSi samples with ~1% Ge, which substitutes Si and results in an increase of the lattice parameter, thus inducing negative pressure on the sample. The structural and magnetic properties of all thus synthesized samples are very similar to each other, and we show the data of an arbitrary chosen sample taken as an example.

The magnetic properties of the samples were first probed with Superconducting Quantum Interference Device (SQUID) magnetometry. Figure 2(a) shows the temperature dependence of the susceptibility χ. We also plotted the first derivative of the susceptibility on the temperature $d\chi/dT$ to emphasize the inflection points $T_c = 39$ K and $T^* = 43$ K on the $\chi(T)$ dependence. These inflection points split the temperature scale into the three regions: (i) an ordered phase from low temperatures to the maximum of $d\chi/dT$; (ii) a critical region between maximum and minimum of $d\chi/dT$; and (iii) the paramagnetic range from the minimum of the first derivative $d\chi/dT$ to higher temperatures. The temperature dependence of the reciprocal susceptibility $1/\chi$ demonstrates a Curie-Weiss law in the paramagnetic range for $T > T^*$.

A small-angle neutron scattering (SANS) investigation has been performed to characterize the magnetic structure of the sample. The SANS experiments were carried out at the SANS-2 scattering facility of the FRG-1 research reactor in Geesthacht (Germany). A typical example of the magnetic scattering at $T = 30$ K (i.e., below T_c) shows the presence of several spots on a ring of intensity, which indicates the coexistence of a number of different spiral domains with differently oriented helix wave vectors $\mathbf{k}$. The value of the wave vector $\mathbf{k}$ is equal to 0.0385 Å^{-1} at low temperatures and increases to 0.0400 Å^{-1} close to T_C. The temperature dependence of the integral SANS intensity of the ring is shown in Fig. 2(b). The intensity of reflection increases upon decrease of the temperature. The extrapolation of the T dependence of the intensity yields the critical temperature $T_C = 39$ K. Thus, in the low-T region the Bragg peaks evidence a spiral magnetic structure, which disappears at $T_C = 39$ K coinciding with the temperature of the maximum of $d\chi/dT$ [Fig. 2(a)], similar to what is reported in Ref. 25 for $Mn_{1-x}Fe_xSi$ compounds.

As is well known[13,30] the magnetic field strongly affects the helical structure of the pure MnSi system. The transitions under an applied magnetic field are very typical for all compounds under study as well as for ideal MnSi. The magnetization curves have been measured at various temperatures below $T_C = 39$ K (Fig. 3). The curves saturate at the critical field H_{C2}, indicating the field-induced phase transition from the conical to the ferromagnetic state.

In the SANS experiment the magnetic field was oriented perpendicular to the incident beam and ranged from 0 to 300 mT. The schematic outline of the experiment can be found in Ref. 13 (see Fig. 4). In the scattering picture these transformations are observable at first as an accumulation of the intensity of the different Bragg spots (forming a ring) into two spots with $\pm\mathbf{k}$ aligned parallel to the field. The threshold field H_{C1} of the first transition can be defined as the field which suppresses the crystalline anisotropy and forms a single domain of conical spirals. With further increase of the magnetic field up to H_{C2}, the conical state transforms into a ferromagnetic spin alignment and the Bragg reflections disappear.

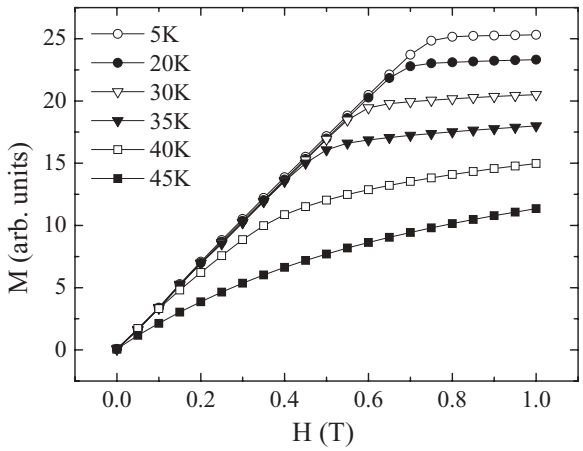

FIG. 3. Magnetic field dependence of the magnetization M taken at $T = 5$, 20, 30, 35, 40, and 45 K for the Ge-doped sample.

An interesting feature in the magnetic field behavior occurs close to T_c, where spin helices with $\mathbf{k} \parallel \mathbf{H}$ transform into a 2D structure with $\mathbf{k} \perp \mathbf{H}$. In the neutron diffraction experiment it is observed as a decrease of intensity of the Bragg reflection at $\mathbf{Q} = \mathbf{k} \parallel \mathbf{H}$, while a new Bragg spot appears at $\mathbf{k} \perp \mathbf{H}$. The typical SANS patterns for the **k**-flop phase is shown in the insets of Fig. 4. The integral intensity of the Bragg reflection (at $\mathbf{k} \parallel \mathbf{H}$) shows a minimum at $H_A = 220$ mT (Fig. 4). The maximum of the scattering intensity at $\mathbf{q} = \mathbf{k} \perp \mathbf{H}$ appears at the same field $H_A = 220$ mT. For the measurements performed in the zero-field cooling regimes the A phase is observed in the field scans down to the temperature $T = 27$ K. The temperature dependence of the SANS intensity taken in the Field Cooled (FC) regime at $H = 232$ mT is shown in Fig. 5. The maps of the SANS intensity at $T = 12$, 16, 20, and 36 K (insets in Fig. 5) demonstrate that the A phase remains observable towards the lowest temperature measured, $T = 12$ K.

The experimental findings on the magnetic structure of the sample under study are summarized in the H-T phase diagram (Fig. 6). The schematic outline of the H-T phase diagram for pure MnSi is given in Fig. 6(a) for comparison. The critical

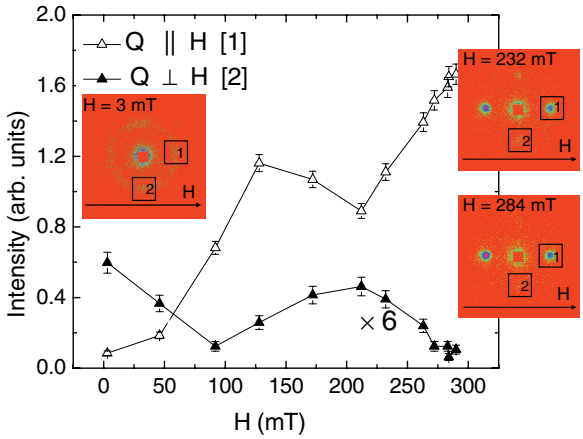

FIG. 4. (Color online) Field dependence of the integral intensity of the Bragg peak at ($\mathbf{k} \parallel \mathbf{H}$) and ($\mathbf{k} \perp \mathbf{H}$) for the doped MnSi sample at $T = 30$ K (a) and $T = 37$ K (b). Insets: Maps of the polarized SANS intensities under magnetic field $H = 3$, 232, and 284 mT.

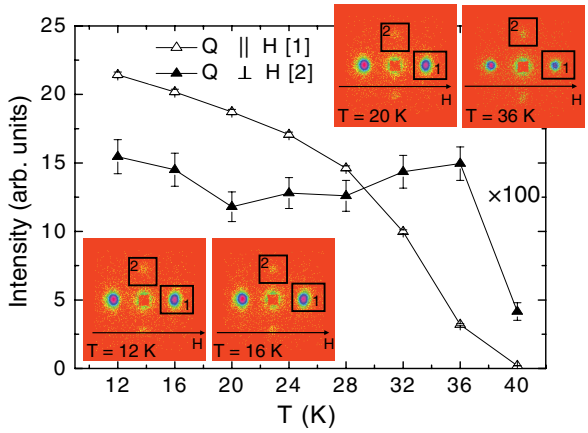

FIG. 5. (Color online) The temperature dependence of the integral SANS intensity at $\mathbf{k} \parallel \mathbf{H}$ and $\mathbf{k} \perp \mathbf{H}$ for the doped MnSi sample at $H = 232$ mT (FC regime). Insets: Maps of the SANS intensity at $T = 12$, 16, 20, and 36 K.

fields H_{C1} obtained from the SANS data and H_{C2} taken from the SQUID data are plotted in Fig. 6(b) as a function of temperature. The critical field H_{C1} is twice as large for doped MnSi sample as for pure MnSi in the whole temperature range below T_C. The field H_{C2} is 25–30% larger than the same value for pure MnSi. As was noticed already the critical temperature T_C for doped MnSi is 30% higher than for pure MnSi.

More dramatic changes are detected in the range of the A phase. Although the A phase is observed for both samples, it is spread over a much wider temperature range for the doped MnSi sample (from 27 K to $T_C = 39$ K) than for pure MnSi

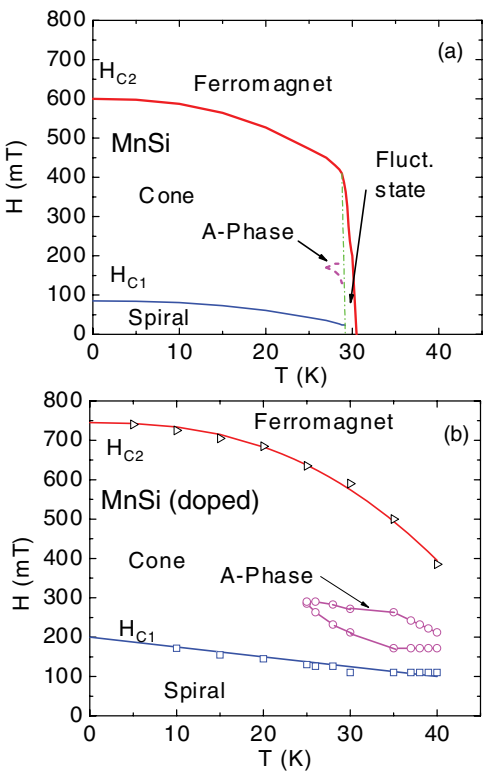

FIG. 6. (Color online) The H-T phase diagrams for the ideal MnSi sample (a) and the doped MnSi sample (b).

(from 27 K to $T_C = 29$ K). It is interesting to note that the lower boundary of the A phase is the same for both compared compounds. The field-cooled procedure leads to the situation in which the A phase structure (with $\mathbf{k} \perp \mathbf{H}$) is pulled down to low temperatures, as was observed for the mixed system $Fe_{1-x}Co_xSi$.[15]

In conclusion, we have shown that the samples of MnSi with chemically induced negative pressure show an increase of the ordering temperature T_C to values comparable to those of thin films. Such an increase of T_C in bulk samples is driven by the Ge doping in MnSi. As is well known, the values of H_{C2} and $\mathbf{k}$ are related to the major driving interactions of the magnetic system, such as the spin wave stiffness $A = g\mu_B H_{C2}/k^2$ and the Dzyaloshinskii constant $SD = Ak$.[31–33] The calculated energies of the principal interactions A/a^2 are equal to 50 meVÅ^2 for the doped and ideal samples, whereas the product SD/a is 10% larger for the doped compound. As the lattice parameter a does not change considerably and the Dzyaloshinskii-Moriya (DM) constant depends only on the B20 structure,[34] one can conclude that the change is related to the average spin value. Thus, the negative pressure leads to an increase of the average spin of the sample, which affects directly the critical temperature T_C and the critical field H_{C2}. These findings are in good agreement with those observed for the MnSi thin films on the Si substrate.[26–28]

We are grateful to V. K. Ivanov (IPNC RAS) for help measuring the sample composition. Special thanks are owed to Yu. B. Lebed and T. S. Clementyev for help with the x-ray diffraction measurements. This work was performed within the framework of the Federal Special Scientific and Technical Program (Projects No. 02.740.11.0874 and No. 07.514.12.4003). The PNPI team acknowledges HZG for their hospitality. The work is partly supported by the RFBR Project No. 10-02-01205-a.

[1] C. Pfleiderer, G. J. McMullan, S. R. Julian, and G. G. Lonzarich, Phys. Rev. B **55**, 8330 (1997).
[2] C. Pfleiderer, S. R. Julian, and G. G. Lonzarich, Nature (London) **414**, 427 (2001).
[3] C. Pfleiderer, D. Resnik, L. Pintschovius, H. Von Lohneysen, M. Garst, and A. Rosch, Nature (London) **427**, 227 (2004).
[4] C. Thessieu, C. Pfleiderer, A. N. Stepanov, and J. Flouquet, J. Phys.: Condens. Matter **9**, 6677 (1997).
[5] S. M. Stishov, A. E. Petrova, S. Khasanov, G. K. Panova, A. A. Shikov, J. C. Lashley, D. Wu, and T. A. Lograsso, Phys. Rev. B **76**, 052405 (2007).
[6] B. Fak, R. A. Sadykov, J. Flouquet, and G. Lapertot, J. Phys.: Condens. Matter **17**, 1635 (2005).
[7] S. V. Grigoriev, S. V. Maleyev, A. I. Okorokov, Yu. O. Chetverikov, R. Georgii, P. Böni, D. Lamago, H. Eckerlebe, and K. Pranzas, Phys. Rev. B **72**, 134420 (2005).
[8] C. Pappas, E. Lelievre-Berna, P. Falus, P. M. Bentley, E. Moskvin, S. Grigoriev, P. Fouquet, and B. Farago, Phys. Rev. Lett. **102**, 197202 (2009).
[9] S. V. Grigoriev, S. V. Maleyev, E. V. Moskvin, V. A. Dyadkin, P. Fouquet, and H. Eckerlebe, Phys. Rev. B **81**, 144413 (2010).
[10] C. Pappas, E. Lelievre-Berna, P. Bentley, P. Falus, P. Fouquet, and B. Farago, Phys. Rev. B **83**, 224405 (2011).
[11] S. V. Grigoriev, E. V. Moskvin, V. A. Dyadkin, D. Lamago, T. Wolf, H. Eckerlebe, and S. V. Maleyev, Phys. Rev. B **83**, 224411 (2011).
[12] A. Hamann, D. Lamago, Th. Wolf, H. V. Lohneysen, and D. Reznik, Phys. Rev. Lett. **107**, 037207 (2011).
[13] S. V. Grigoriev, S. V. Maleyev, A. I. Okorokov, Yu. O. Chetverikov, and H. Eckerlebe, Phys. Rev. B **73**, 224440 (2006).
[14] S. Muhlbauer, B. Binz, F. Jonietz, C. Pfeiderer, A. Rosch, A. Neubauer, R. Georgii, and P. Boni, Science **323**, 915 (2009).
[15] C. Pfeiderer, T. Adams, A. Bauer, W. Biberacher, B. Binz, F. Birkelbach, P. Boni, C. Franz, R. Georgii, M. Janoschek *et al.*, J. Phys.: Condens. Matter **22**, 164207 (2010).
[16] S. V. Grigoriev, D. Chernyshov, V. A. Dyadkin, V. Dmitriev, S. V. Maleyev, E. V. Moskvin, D. Menzel, J. Schoenes, and H. Eckerlebe, Phys. Rev. Lett. **102**, 037204 (2009).
[17] S. V. Grigoriev, D. Chernyshov, V. A. Dyadkin, V. Dmitriev, E. V. Moskvin, D. Lamago, Th. Wolf, D. Menzel, J. Schoenes, S. V. Maleyev, and H. Eckerlebe, Phys. Rev. B **81**, 012408 (2010).
[18] V. A. Dyadkin, S. V. Grigoriev, D. Menzel, E. V. Moskvin, S. V. Maleyev, and H. Eckerlebe, Phys. B (Amsterdam, Neth.) **406**, 2385 (2011).
[19] V. A. Dyadkin, S. V. Grigoriev, D. Menzel, D. Chernyshov, V. Dmitriev, J. Schoenes, S. V. Maleyev, E. V. Moskvin, and H. Eckerlebe, Phys. Rev. B **84**, 014435 (2011).
[20] N. Manyala, Y. Sidis, J. F. DiTusa, G. Aeppli, D. P. Young, and Z. Fisk, Nature (London) **404**, 581 (2000).
[21] N. Manyala, Y. Sidis, J. F. DiTusa, G. Aeppli, D. P. Young, and Z. Fisk, Nat. Mater. **3**, 255 (2004).
[22] B. Lebech, J. Bernhard, and T. Freltoft, J. Phys.: Condens. Matter **1**, 6105 (1989).
[23] S. V. Grigoriev, S. V. Maleyev, E. V. Moskvin, V. A. Dyadkin, P. Fouquet, and H. Eckerlebe, Phys. Rev. B **81**, 144413 (2010).
[24] A. Bauer, A. Neubauer, C. Franz, W. Münzer, M. Garst, and C. Pfleiderer, Phys. Rev. B **82**, 064404 (2010).
[25] S. V. Grigoriev, E. V. Moskvin, V. A. Dyadkin, D. Lamago, T. Wolf, H. Eckerlebe, and S. V. Maleyev, Phys. Rev. B **83**, 224411 (2011).
[26] E. Karhu, S. Kahwaji, T. L. Monchesky, C. Parsons, M. D. Robertson, and C. Maunders, Phys. Rev. B **82**, 184417 (2010).
[27] E. A. Karhu, S. Kahwaji, M. D. Robertson, H. Fritzsche, B. J. Kirby, C. F. Majkrzak, and T. L. Monchesky, Phys. Rev. B **84**, 060404(R) (2011).
[28] E. A. Karhu, U. K. Rossler, A. N. Bogdanov, S. Kahwaji, B. J. Kirby, H. Fritzsche, M. D. Robertson, C. F. Majkrzak, and T. L. Monchesky, Phys. Rev. B **85**, 094429 (2012).
[29] B. Fak, R. A. Sadykov, J. Flouquet, and G. Lapertot, J. Phys.: Condens. Matter **17**, 1635 (2005).
[30] S. V. Grigoriev, S. V. Maleyev, A. I. Okorokov, Yu. O. Chetverikov, P. Boni, R. Georgii, D. Lamago, H. Eckerlebe, and K. Pranzas, Phys. Rev. B **74**, 214414 (2006).
[31] S. V. Maleyev, Phys. Rev. B **73**, 174402 (2006).
[32] S. V. Grigoriev, V. A. Dyadkin, D. Menzel, J. Schoenes, Yu. O. Chetverikov, A. I. Okorokov, H. Eckerlebe, and S. V. Maleyev, Phys. Rev. B **76**, 224424 (2007).
[33] S. V. Grigoriev, S. V. Maleyev, V. A. Dyadkin, D. Menzel, J. Schoenes, and H. Eckerlebe, Phys. Rev. B **76**, 092407 (2007).
[34] S. V. Grigoriev, V. A. Dyadkin, E. V. Moskvin, D. Lamago, T. Wolf, H. Eckerlebe, and S. V. Maleyev, Phys. Rev. B **79**, 144417 (2009).